

Transport induced by Density Waves in a Andreev-Lifshitz Supersolid

Kwang-Hua W. Chu [*]

P.O. Box 30-15, Shanghai 200030, PR China

Abstract

Macroscopic derivation of the entrainment in a Andreev-Lifshitz Supersolid induced by a surface elastic wave propagating along the flexible interface is conducted by considering the nonlinear coupling between the interface and the rarefaction effect. We obtain the critical bounds for zero-volume-flow-rate states corresponding to specific rarefaction measure and wave number which is relevant to the rather small critical velocity of supersolid flows reported by Kim and Chan.

KEY WORDS : quantum crystal, surface phonon, freezing

PACS numbers:

In 1969, it was conjectured by Andreev and Lifshitz¹ that at zero temperature, delocalized defects may exist in a quantum solid, as a result of which the number of sites of an ideal crystal lattice may not coincide with the total number of particles. Originally, this conjecture was proposed for three dimensional quantum solids made of atoms (^3He , ^4He , ...) which do not interact via Coulomb repulsion. The proposed *supersolid* phase is believed to occur due to the quantum behavior of point defects, namely vacancies and interstitials, in this crystal of bosons²⁻³. Researchers have found that a small lattice model does not exhibit the mesoscopic signature of an intermediate phase separating the solid from the liquid, where the solid and the fluid would coexist⁴. Such a vacancy-solid phase was indeed suggested¹ by Andreev and Lifshitz if the zero point motions of certain defects become sufficient to form waves propagating inside the solid.

Castaing and Nozières have later considered⁵ such a possibility for spin polarized ^3He . The statistics of the defects depend on their nature. For simple vacancies in the crystal, their statistics is given by the statistics of the particles out of which the solid is made. If the defects are bosons, they may form a condensate, giving rise to a superfluid coexisting with the solid. This supersolid phase is discussed in certain bosonic models⁶. If the defects are fermions, they may form a Fermi liquid⁷ coexisting with the solid, such that the system is neither a solid, nor a liquid. Two kinds of motion are possible in it; one possesses the properties of motion in an elastic solid, the second possesses the properties of motion in a liquid. This interesting issue motivates our present study.

Early theoretical work by Andreev and Lifshitz¹ and Chester² showed that solids may feature a Bose-Einstein condensate of vacancies (or interstitial atoms) and thus possess superfluid (SF) properties. Quite recently one description of the quantum solid is as a density wave that has formed in the quantum fluid⁸⁻⁹. The periodicity of this density wave need not match precisely to the particle density, so that the ground state may be incommensurate, with unequal densities of vacancies and interstitials. Whether or not the same is true for quantum *fluctuations* is not clear at this point. We noticed that previous theories imply a corresponding vacancy contribution to the specific heat that is as large as the phonon contribution near 1 Kelvin^{3,10}. Based on these considerations or phenomenological approaches, in this letter, we shall demonstrate that wavy flexible interface (between atoms and free vacancies or defects) or highly-pressured environments⁸ can produce elastically deformed interface or peristaltic motion will induce time-averaged transport in a Andreev-Lifshitz supersolid.

Theoretical studies of interphase nonlocal transport phenomena which appear as a result of a different type of nonequilibrium representing propagation of a surface elastic wave have been performed before^{11–12}. These are relevant to particles flowing along deformable elastic slabs with the dominated parameter being the Knudsen number ($\text{Kn} = \text{mean-free-path}/L_d$, mean-free-path (mfp) is the mean free path of the particles, L_d is proportional to the distance between two slabs)^{13–15}. The role of the Knudsen number is similar to that of the Navier slip parameter $N_s (= \mu S/L_d$; S is a proportionality constant as $u_s = S\tau$, τ : the shear stress of the bulk velocity; u_s : the dimensional slip velocity; for a no-slip case, $S = 0$, but for a no-stress condition. $S = \infty$, μ is the viscosity).

We shall choose a periodic domain to simplify our mathematical treatments. The flat interface is presumed. We adopt the macroscopic or hydrodynamical approach and simplify the original system of equations (related to the momentum and mass transport) to one single higher-order quasi-linear partial differential equation in terms of the unknown stream function. In this study, as the temperature is rather low and the phase is related to the supersolid (there might be weakly friction or shearing dissipation in-between) we shall assume that the governing equations are the incompressible Navier-Stokes equations which will be associated with the microscopically slip velocity boundary conditions along the interfaces^{13–15}. To consider the originally quiescent environment for simplicity, due to the difficulty in solving a fourth-order quasi-linear complex ordinary differential equation (when the wavy boundary condition are imposed), we can finally get an analytically perturbed solution and calculate those physical quantities, like, time-averaged transport or entrainment, critical forcing corresponding to the freezed or zero-volume-flow-rate states.

We consider a two-dimensional region of uniform thickness. The flat-plane boundaries or interfaces are rather flexible and presumed to be elastic, on which are imposed traveling sinusoidal waves of small amplitude a (possibly due to quantum fluctuations). The vertical displacements of the upper and lower interfaces ($y = L_d$ and $-L_d$) are thus presumed to be η and $-\eta$, respectively, where $\eta = a \cos[2\pi(x - ct)/\lambda]$, λ is the wave length, and c the wave speed. x and y are Cartesian coordinates, with x measured in the direction of wave propagation and y measured in the direction normal to the mean position of the interfaces. We have a characteristic velocity c and three characteristic lengths a , λ , and L_d . The following variables based on c and L_d could thus be introduced: $x' = x/L_d$, $y' = y/L_d$, $u' = u/c$, $v' = v/c$, $\eta' = \eta/L_d$, $\psi' = \psi/(cL_d)$, $t' = ct/h$, $p' = p/(\rho c^2)$, where ψ is the dimensional

stream function, u and v are the velocities along the x - and y -directions; ρ is the density, p is the pressure. The primes could be dropped in the following. The amplitude ratio ϵ , the wave number α , and the Reynolds number Re (representing the weakly friction or shearing dissipation using a viscosity ν) are defined by $\epsilon = a/L_d$, $\alpha = 2\pi L_d/\lambda$, $Re = c L_d/\nu$. We shall seek a solution in the form of a series in the small parameter ϵ : $\psi = \psi_0 + \epsilon\psi_1 + \epsilon^2\psi_2 + \dots$, $\partial p/\partial x = (\partial p/\partial x)_0 + \epsilon(\partial p/\partial x)_1 + \epsilon^2(\partial p/\partial x)_2 + \dots$, with $u = \partial\psi/\partial y$, $v = -\partial\psi/\partial x$. The 2D (x - and y -) momentum equations and the equation of continuity¹⁶⁻¹⁷ could be in terms of the stream function ψ if the p -term is eliminated. The final governing equation is

$$\frac{\partial}{\partial t}\nabla^2\psi + \psi_y\nabla^2\psi_x - \psi_x\nabla^2\psi_y = \frac{1}{Re}\nabla^4\psi, \quad \nabla^2 \equiv \frac{\partial^2}{\partial x^2} + \frac{\partial^2}{\partial y^2}, \quad (1)$$

and subscripts indicate the partial differentiation. Thus, we have

$$\frac{\partial}{\partial t}\nabla^2\psi_0 + \psi_{0y}\nabla^2\psi_{0x} - \psi_{0x}\nabla^2\psi_{0y} = \frac{1}{Re}\nabla^4\psi_0, \quad (2)$$

$$\frac{\partial}{\partial t}\nabla^2\psi_1 + \psi_{0y}\nabla^2\psi_{1x} + \psi_{1y}\nabla^2\psi_{0x} - \psi_{0x}\nabla^2\psi_{1y} - \psi_{1x}\nabla^2\psi_{0y} = \frac{1}{Re}\nabla^4\psi_1, \quad (3)$$

and other higher order terms. Microscopic boundary conditions imposed by the symmetric motion of the interfaces and the non-zero slip velocities¹³⁻¹⁴ are : $u = \mp Kn \, du/dy$, $v = \pm\partial\eta/\partial t$ at $y = \pm(1 + \eta)$, here $Kn = mfp/L_d$. The boundary conditions are expanded in powers of η and then ϵ . These equations, together with the condition of symmetry and a uniform $(\partial p/\partial x)_0$, yield : $\psi_0 = K_0[(1 + 2Kn)y - y^3/3]$, $K_0 = Re(-\partial p/\partial x)_0/2$, $\psi_1 = \{\phi(y)e^{i\alpha(x-t)} + \phi^*(y)e^{-i\alpha(x-t)}\}/2$, where the asterisk denotes the complex conjugate. A substitution of ψ_1 into Eqn. (3) yields

$$\left\{\frac{d^2}{dy^2} - \alpha^2 + i\alpha Re[1 - K_0(1 - y^2 + 2Kn)]\right\}\left(\frac{d^2}{dy^2} - \alpha^2\right)\phi - 2i\alpha K_0 Re \phi = 0$$

or if originally the environment is quiescent : $K_0 = 0$ (this corresponds to a free pumping case) $(d^2/dy^2 - \alpha^2)(d^2/dy^2 - \bar{\alpha}^2)\phi = 0$, $\bar{\alpha}^2 = \alpha^2 - i\alpha Re$. The boundary conditions are $\phi_y(\pm 1) \pm \phi_{yy}(\pm 1)Kn = 0$, $\phi(\pm 1) = \pm 1$. Similarly, with $\psi_2 = \{D(y) + E(y)e^{i2\alpha(x-t)} + E^*(y)e^{-i2\alpha(x-t)}\}/2$, we have much more complicated equations (cf. Chu in [17]) and the boundary conditions

$$D_y(\pm 1) + \frac{1}{2}[\phi_{yy}(\pm 1) + \phi_{yy}^*(\pm 1)] = \mp Kn\left\{\frac{1}{2}[\phi_{yyy}(\pm 1) + \phi_{yyy}^*(\pm 1)] + D_{yy}(\pm 1)\right\}, \quad (4)$$

$E_y(\pm 1) + \phi_{yy}(\pm 1)/2 = \mp Kn[\phi_{yyy}(\pm 1)/2 + E_{yy}(\pm 1)]$, $E(\pm 1) + \phi_y(\pm 1)/4 = 0$. After lengthy algebraic manipulations, we obtain $\phi = c_0 e^{\alpha y} + c_1 e^{-\alpha y} + c_2 e^{\bar{\alpha} y} + c_3 e^{-\bar{\alpha} y}$, where $c_i, i = 0, 1, 2, 3$

are related to α , $\bar{\alpha}$, and Kn (cf. Chu in Ref. 17).

To obtain a simple solution which relates to the mean transport so long as only terms of $O(\epsilon^2)$ are concerned, we see that if every term in the x-momentum equation is averaged over an interval of time equal to the period of oscillation, we obtain

$$\overline{\frac{\partial p}{\partial x}} = \epsilon^2 \overline{\left(\frac{\partial p}{\partial x}\right)_2} = \epsilon^2 \left[\frac{D_{yyy}}{2Re} + \frac{iRe}{4} (\phi \phi_{yy}^* - \phi^* \phi_{yy}) \right] + O(\epsilon^3) = \epsilon^2 \frac{\Pi_0}{Re} + O(\epsilon^3), \quad (5)$$

where Π_0 is the integration constant and could be fixed indirectly in the coming equation below. Now, from Eqn. (4), we have

$$D_y(\pm 1) \pm \text{Kn} D_{yy}(\pm 1) = -\frac{1}{2} [\phi_{yy}(\pm 1) + \phi_{yy}^*(\pm 1)] \mp \text{Kn} \left\{ \frac{1}{2} [\phi_{yyy}(\pm 1) + \phi_{yyy}^*(\pm 1)] \right\}, \quad (6)$$

where $D_y(y) = \Pi_0 y^2 + a_1 y + a_2 + \mathcal{C}(y)$, and together from the expression of ψ_2 , we can obtain $\mathcal{C}(y)$ which also depends on the α , $\bar{\alpha}$, Re , c_i , $i = 0, 1, 2, 3$ (cf. Chu in Ref. 17). In realistic applications we must determine Π_0 from considerations of outlet conditions of the slab-region. a_1 equals to zero because of the symmetry of boundary conditions.

Once Π_0 is specified, our solution for the mean speed (u averaged over time) of superflow is $U = \epsilon^2 D_y / 2 = \epsilon^2 \{ \mathcal{C}(y) - \mathcal{C}(1) + R_0 - \text{Kn} \mathcal{C}_y(1) + \Pi_0 [y^2 - (1 + 2\text{Kn})] \} / 2$ where $R_0 = -\{ [\phi_{yy}(1) + \phi_{yy}^*(1)] - \text{Kn} [\phi_{yyy}(1) + \phi_{yyy}^*(1)] \} / 2$. To illustrate our results clearly, we adopt $U(Y) \equiv u(y)$ for the time-averaged results with $y \equiv Y$ in the following.

Our numerical calculations confirm that the mean streamwise velocity distribution (averaged over time) due to the induced motion by the wavy elastic interface in the case of free (vacuum) pumping is dominated by R_0 (or Kn) and the parabolic distribution $-\Pi_0(1 - y^2)$. R_0 which defines the boundary value of D_y has its origin in the y-gradient of the first-order streamwise velocity distribution. Note that the Reynolds number here is based on the wave speed. The physical trend herein is also the same as those reported before^{13–14,17} for the slip-flow effects. The slip produces decoupling with the inertia of the wavy interface.

Now, let us define a critical reflux condition as one for which the mean velocity $U(Y)$ equals to zero at the center-line $Y = 0$. With the equation of U , we have $\Pi_{0_{cr}} = \overline{Re(\partial p / \partial x)_2} = -[\alpha^2 Re^2 F(0) / 200 + \text{Kn} \mathcal{C}'(1) - R_0] / (1 + 2\text{Kn})$ which means the critical reflux condition is reached when Π_0 has above value. Pumping against a positive forcing greater than the critical value would result in a backward transport (reflux) in the central region of the stream. This critical value depends on α , Re , and Kn . There will be no reflux if the pressure gradient is smaller than this Π_0 . Thus, for some Π_0 values less than $\Pi_{0_{cr}}$, the superflow will keep

moving forward. On the contrary, parts of the flow will move backward if $\Pi_0 > \Pi_{0_{cr}}$.

As reported in Ref. 8, the rather small critical velocity ($\leq 20\mu\text{m/s}$) observed shows an apparent dissipation or attenuation of the superflow. Thus, we present some of the values of $\Pi_0(\alpha, Re; \text{Kn} = 0, 0.1)$ corresponding to freezed or zero-volume-flow-rate states ($\int_{-1}^1 U(Y)dY = 0$) in Table 1 where the wave number (α) has the range between 0.10 and 0.90; the Reynolds number (Re) = 0.1, 1, 10, 50, 100. We observe that as Kn increases from zero to 0.1, the critical Π_0 decreases significantly (cf. Fig. 1). For the same Kn , once Re is larger than 10, critical reflux values Π_0 drop rapidly and the wave-modulation effect (due to α) appears. The latter observation might be interpreted as the strong coupling between the interface and the inertia of the streaming superflow. The illustration of the velocity fields for those zero-flux (zero-volume-flow-rate) or freezed states are shown in Figure 2. There are three wave numbers : $\alpha = 0.2, 0.5, 0.8$. The Reynolds number is 50. Both no-slip and slip ($\text{Kn}=0.1$) cases are presented. The arrows for slip cases are schematic and represent the direction of positive and negative velocity fields.

Some remarks could be made about these states : the transport being freezed in the time-averaged sense for specific dissipations (in terms of Reynolds number which is the ratio of wave-inertia and viscous shearing effects) and wave numbers (due to the wavy interface or vacuum fluctuations) for either no-slip and slip cases. Meanwhile, the time-averaged transport induced by the wavy interface is proportional to the square of the amplitude ratio (although the small amplitude waves being presumed), as can be seen in Eqn. (5), which is qualitatively the same as that presented in Ref. 11 for analogous interfacial problems.

In brief summary, the entrained transport (either positive or negative and there is possibility : freezing) due to the wavy interface is mainly tuned by the Π_0 for fixed Re . Meanwhile, $\Pi_{0_{cr}}$ depends strongly on the Knudsen number (Kn , a rarefaction measure) instead of Re or α . These results (cf. Table 1 and Fig. 1) might explain why there are rather small critical velocities for superflows in the temperature range where a supersolidity is observed⁸. Finally we like to stress that once the phase is solid then the elastically tensile stress should be larger than that of the liquid phase and the latter could be a crucial test for the existence of the supersolidity.

[*] Correspondence after 2007-Aug-30 : 24, Lane 260, Section 1, Road Mucha, Taipei 11646,

Taiwan, R. China and P.O. Box 39, Tou-Di-Ban, Road XiHong, Urumqi 830000, PR China.

- [1] A.F. Andreev and I.M. Lifshitz, Zh. Eksp. Teor. Fiz. (Sov. Phys. JETP) **29**, 1107 (1969).
- [2] G.V. Chester, Phys. Rev. A **2**, 256 (1970).
- [3] P.W. Anderson, W.F. Brinkman, and D.A. Huse, Science **310**, 1164 (2005).
- [4] G. Katomeris, F. Selva, and J.-L. Pichard, Eur. Phys. J. B **31**, 401 (2003). Z.Á. Németh and J.-L. Pichard, Eur. Phys. J. B **33**, 87 (2003).
- [5] B. Castaing and P. Nozières, J. Phys. France **40**, 257 (1979)
- [6] G.G. Batrouni, R.T. Scalettar, Phys. Rev. Lett. **84**, 1599 (2000).
- [7] I.E. Dzyaloshinskii, P.S. Kondratenko, V.S. Levchenkov, Sov. Phys. JETP **35**, 823 (1972);
ibid. **35**, 1213 (1972).
- [8] A.C. Clark and M.H.W. Chan, J. Low Temp. Phys. **138**, 853 (2005). E. Kim and M.H.W. Chan, J. Low Temp. Phys. **138**, 859 (2005).
- [9] T. Leggett, Science **305**, 1921 (2004). Z.Á. Németh and J.-L. Pichard, Eur. Phys. J B **45**, 111 (2005). A.T. Dorsey, P.M. Goldbart and J. Toner, Phys. Rev. Lett. **96**, 055301 (2006).
- [10] C.A. Burns and J.M. Goodkind, J. Low Temp. Phys. **95**, 695 (1994).
- [11] V.D. Borman, S.Yu. Krylov, and A.M. Kharitonov, Sov. Phys. JETP **65**, 935 (1987).
- [12] M.S. Longuet-Higgins, Philos. Trans. R. Soc. London **345**, 535 (1953). K.-H. W. Chu, J. Phys. A : Math. General. **36**, 5817 (2003).
- [13] D. Einzel and J.M. Parpia, J. Low Temp. Phys. **109**, 1 (1997).
- [14] M.N. Kogan, *Rarefied Gas Dynamics* (Plenum Press, New York, 1969).
- [15] P.G. de Gennes, Langmuir **18**, 3013 (2002).
- [16] L.D. Landau and E.M. Lifshitz, *Fluid Mechanics* (Pergamon Press, London, 1959). C. Truesdell, Am. Math. Monthly **60**, 445 (1953).
- [17] K.-H. W. Chu, Phys. Scr. **65**, 283 (2002). K.-H. W. Chu, submitted for publication (2006).

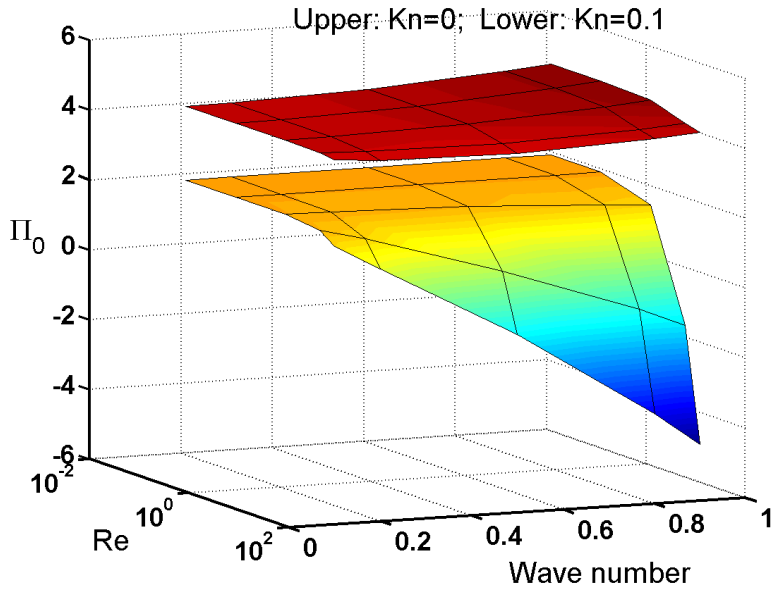


Fig. 1 Demonstration of Kn , Re and α effects on the Π_0 (zero-flux states).

Re is the Reynolds number (the ratio of the wave-inertia and viscous shearing dissipation).

α is the wave number and Kn is the Knudsen number (a rarefaction measure).

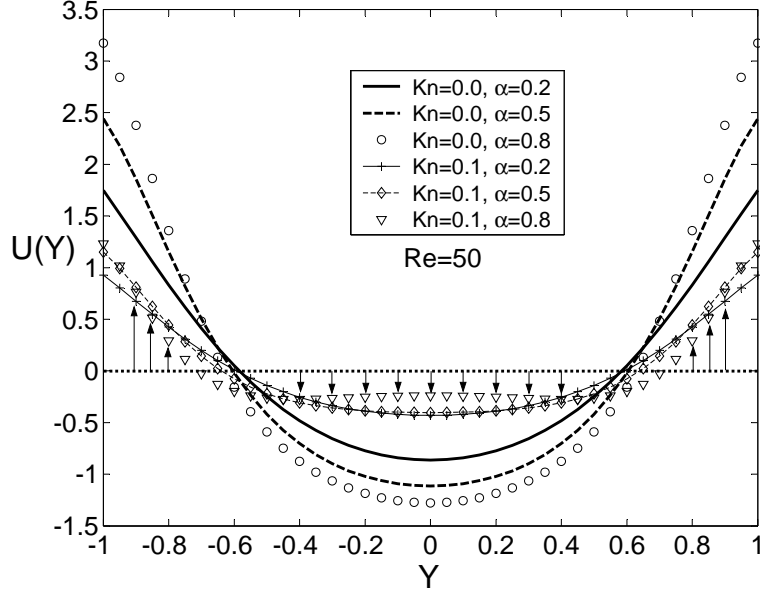


Fig. 2 Demonstration of the zero-flux states : the mean velocity field $U(Y)$ for wave numbers $\alpha = 0.2, 0.5, 0.8$. The Reynolds number is 50. Kn is the rarefaction measure (the mean free path of the particles divided by the characteristic length). The arrows are schematic and illustrate the directions of positive and negative $U(Y)$. The integration of $U(Y)$ w.r.t. Y for these velocity fields gives zero volume flow rate.

TABLE I: Zero-flux or freezed states values (Π_0) for a flat wavy interface.

		Re				
Kn	α	0.1	1	10	50	100
0	0.1	4.5088	4.5087	4.5078	4.4863	4.4316
	0.2	4.5269	4.5269	4.5231	4.4496	4.3275
	0.5	4.6586	4.6584	4.6359	4.4086	4.2682
	0.8	4.9238	4.9234	4.8708	4.5714	4.4488
	0.9	5.0475	5.0468	4.9827	4.6709	4.5516
0.1	0.1	2.3983	2.3982	2.3927	2.2676	1.9560
	0.2	2.4003	2.4000	2.3774	1.9532	1.2217
	0.5	2.4149	2.4132	2.2731	0.7728	-0.9054
	0.8	2.4422	2.4379	2.0718	-0.5885	-3.4151
	0.9	2.4542	2.4486	1.9825	-1.1191	-4.3972